Modeling of milk acidification

C.E. Robles-Rodriguez * **E. Szymańska** ** **L. Özkan** *

* *Control Systems Group, Department of Electrical Engineering, Eindhoven, The Netherlands (e-mail: c.e.robles.rodriguez@tue.nl, l.ozkan@tue.nl)*
** *FrieslandCampina, Amersfoort, The Netherlands*

Abstract: This paper deals with the development of an empirical model to describe the dynamics of milk acidification process for the production of acid casein. The model is based on the dynamics of the pH profiles during the acidification process since pH is a good indicator of the status of the precipitation. Data from laboratory experiments has been used to identify the parameters in the proposed model. Calibration and validation results, with an independent data set, show that the model is able to predict accurately the pH at different temperatures and acid addition rates. Furthermore, the model has been used in a simulation study as an advisory tool to suggest acid addition, proving the parsimony of the model.

Keywords: Modeling, milk acidification, pH, casein production, parameter estimation.

1. INTRODUCTION

Acidification is an important operation in food industry dealing with the increase of taste, viscosity, and shelf life of dairy products (e.g. milk, yogurt) (Mudgil and Barak, 2019). Regularly, acidification is carried out to decrease the milk pH to 4.6 as compared to natural milk pH (6.6 – 6.8). A major application of acidification in dairy product manufacture is in the production of acid casein, the base material from which caseinates can be prepared. Caseins and caseinates are used as ingredients in a wide variety of food and nonfood products (Sarode et al., 2015).

The industrial production of acid casein follows several unit operations as displayed in Fig.1. The milk is first heated up to 40 – 45^oC and mineral acid is added in a precipitation pipe to bring the pH of the milk around 4.6 in order to generate smooth aggregates of casein. The casein and whey mixture are passed though a decanter before encountering washing to remove the whey. Before leaving the plant, the whey and the wash water can be separated and the casein sludge is collected in a tank. When mixed with a lye solution, the casein dissolves and it is then remixed with the skim milk intended for casein production. After dewatering, the acid casein is ground and packed (TetraPack, 2015).

The main production step is the precipitation, in which acid casein is retrieved via milk acidification. This step depends on several factors such as temperature, aging time, acid addition rates, agitation, etc. Monitoring and regulating precipitation is essential because it determines the initial particle size and the formation of undesired components, such as calcium phosphate. Online monitoring of particle size distribution is complicated. A simple alternative is to monitor pH, which has been presented as a good indicator of the status of precipitation (Lucey, 2017). Hence, the dynamics of pH during acidification can provide information about the quality of acid casein and mathematical models can serve to follow the dynamic behavior.

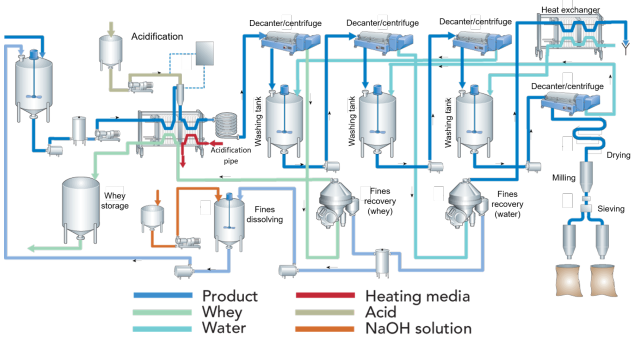

Fig. 1. Casein production process (TetraPack, 2015).

A limited number of mathematical models have been developed for describing pH during milk acidification. The works of Mekmene et al. (2009); Holt (2004) have characterized salt equilibrium in milk acidification. These models are accurate in steady state conditions and they require a lot of calculations about several ionic species. The work of Hofland et al. (2003) studied the dynamics of milk acidification with a model to describe pH profiles considering the electro-neutrality condition, where information about particle size and coagulation times were needed for the calculation of the model. Although accurate, this model is data dependent because it needs to specify the coagulation time. Hence, it is complicated to extend these models for different conditions, especially when there is lack of information.

This paper proposes a model to describe pH during acidification making use of the available data measured online, such as temperature and acid addition rates. The main idea is to propose a simple model to capture the transient behavior of pH at different conditions in a way that it can be used for control purposes (*i.e.*, industrial production).

The remainder of this paper is organized as follows. Section 2 presents the chemistry of milk acidification. Section 3 describes the model development for milk acidification including the assumptions and the experiments that have been considered for its development. Section 4 reports on the calibration and validation of the model. Furthermore, the use of the model is addressed in an example to show potential application towards the control of pH. Finally, section 5 summarizes the results and provides insights on future work.

2. MILK ACIDIFICATION

The precipitation of casein is a complex process that takes into account (i) the mixing of the acid with the milk, (ii) the diffusion of the protons into the micelles, (iii) the diffusion of the dissolved calcium phosphates out of the micelle, (iv) precipitation, and (v) aggregation of the particles (Hofland et al., 2003).

Casein is produced from pasteurized milk (generally skim milk) by acidification, which is mostly achieved by the addition of mineral acids (*i.e.*, hydrochloric, sulfuric acids). When the pH of milk is decreased, the different acido-basic groups of milk's constituents (organic and inorganic phosphate, citrate, carboxylic residues) become increasingly more protonated (De Kruif, 1997). As a consequence, casein micelles coagulate and are released into the diffusible fraction of milk and micellar calcium phosphate is dissolved into the serum. This solubilization is complete at approximately pH 5.0 (Fox, 2011). However, acidification stops when the electrostatic repulsion between casein micelles is reduced and reaches equilibrium at a pH value of ≈ 4.6, which is called isoelectric point (IEP) (Lucey, 2017). At the end of the acidification, two parts are distinguished: the curd (coagulated casein) and the serum which contains the soluble components of skim milk (lactose, whey proteins and minerals, including the colloidal calcium phosphate). Hence, acidification is an efficient method for producing high purity casein powders.

Acidification depends on several factors such as temperature, aging time, acid addition rates, agitation, etc (Holt et al., 1981). Temperature has an effect on the hydrophobic interactions during casein micelle coagulation at pH 4.6 (Jablonka et al., 1986). These hydrophobic interactions are entropically driven and are thus stronger at higher temperatures Bringe and Kinsella (1990). On the contrary, generally at low temperatures (< 10 ^{o}C) no coagulation takes place. Temperature has also influence on the texture of the curd (Sarode et al., 2015). The acid addition rate can also have influence on the particle size of the curd. Bringe and Kinsella (1990) reported that rapid acidification of milk results in rapid casein micelle coagulation forming large and dense aggregates. Hofland et al. (2003) showed that at longer acidification times, the curd spends more time at higher pH-values where precipitation is slow, resulting in finer particles. Another important factor is mixing since stirring is necessary to distribute the acid uniformly (Sarode et al., 2015). Vigorous mixing, however, can induce curd breakup resulting in smaller curd particles (Hofland et al., 2003).

3. MODELING OF MILK ACIDIFICATION

3.1 Experiments

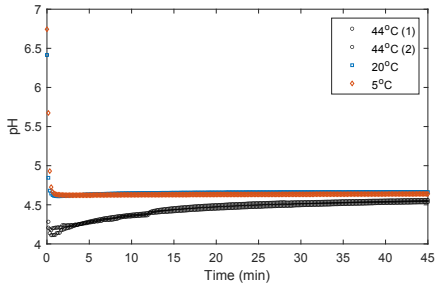

(a) $t_A = 0$ min

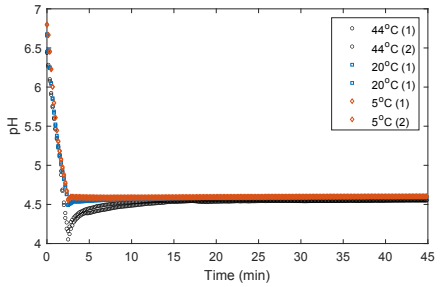

(b) $t_A = 2.5$ min

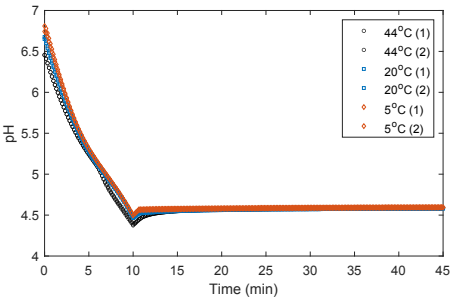

(c) $t_A = 10$ min

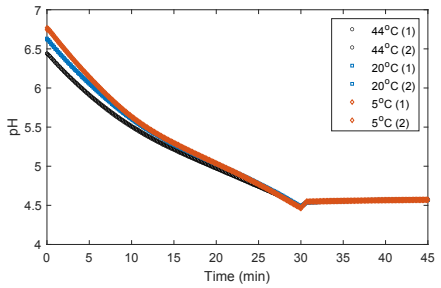

(d) $t_A = 30$ min

Fig. 2. Experimental data for milk acidification at different temperature and acidification times. The numbers in the parenthesis indicate the replicate number.

Several experiments have been carried out to investigate the dynamics of acidification of milk in terms of pH variations. To this end, 150 mL of pasteurized skim milk was equilibrated to a required temperature 5, 20 and 44 ^{o}C. Subsequently, the samples were acidified with a solution of 0.5 M sulfuric acid. A volume of 7.92 mL of H_2SO_4

(A_T) was determined to be sufficient to lower the pH of the 150 mL of skim milk to the isoelectric point of casein (pH $\approx$ 4.6). The acid was added over different acidification times (t_A): 0, 2.5, 10, 30 min, where the acidification rate was defined as $Q_A = A_T/t_A$. The experimental results are displayed in Fig. 2, where pH values were recorded every 10 seconds. From these experiments, two different behaviors are observed: a pH decrease corresponding to an acid addition stage having a duration of t_A, and a stage where pH achieves equilibrium due to diffusion of the remaining acid in the liquid. The replicates of the experiments present an almost exact behavior at temperatures of 5 and 20^{o}C, and at long acidification times ($t_A = 10, 30$ min.). In replicates at 44^{o}C and $t_A = 0, 2.5$ minutes, there are some variations (Fig. 2(a),2(b)) displaying an abrupt decrease of pH followed by a slow increase up to the equilibrium point, which, in this case, is around 4.65 (See Fig. 2(a)). Rapid acidification of milk results in fast casein micelle coagulation forming large aggregates and a less gradual pH decrease (Hofland et al., 2003). When longer acidification rates are used ($t_A = 30$ min.), the pH decreases gradually implying a slow coagulation with no formation of big aggregates.

The effect of temperature is also seen in Fig. 2, where at low temperatures (5^{o}C and 20^{o}C) there is a smooth decrease of pH, which is related to the fact that at low temperatures (<10^{o}C) generally no coagulation takes place at pH 4.6 (Jablonka et al., 1986). Furthermore, in experiments carried out at 44^{o}C the whey was clearly separated from the curd. At 20^{o}C less separation was visible and at 5^{o}C there was no separation.

3.2 Modeling pH dynamics

An empirical model to capture the dynamics of pH is developed based on the measured variables, such as acidification times t_A (min), temperature T (K), the acid addition rate Q_A (L_{acid}/min) and the volume of milk V_{milk} (L_{milk}). For the sake of simplicity, let us define A as,

$$A = \frac{\text{Cumulative volume of added acid}}{\text{Volume of milk}} = \sum \frac{Q_A}{V_{\text{milk}}}$$

which represents the cumulative added acid per volume of milk (L_{acid}/L_{milk}) and can be considered dimensionless.

The modeling approach consists of finding a function ϕ for pH depending on the measured variables in a structured manner, where independent functions $f(\cdot)$ interact. Therefore, the model can be expressed as:

$$\text{pH} = \phi(A, T, t_A) = f(A) \cdot f(T) \cdot f(t_A) \qquad (1)$$

The dynamic model is built based on the experiments reported in the previous subsection. The empirical model distinguishes two main stages: (i) Acid addition ($t \leq t_A$) and (ii) Diffusion ($t > t_A$).

The acid addition stage occurs when acid is being provided in the flask. Within this stage, we have noticed an interesting property in the data. The pH dynamics and the cumulative added acid per volume of milk (A) depict a time invariant relationship for low temperatures and large acidification times. However, when temperature is higher (44^{o}C) the invariant relationship only holds for pH value above 5.1. The invariant relationship is displayed in

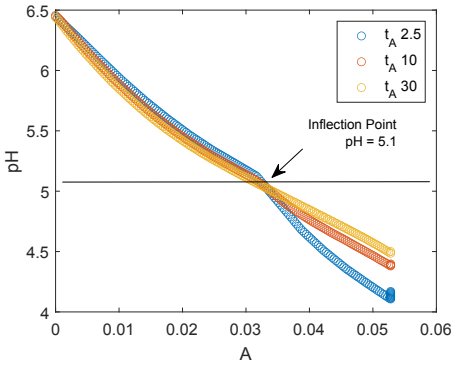

Fig. 3. pH as a function of added acid (A) at 44 ^{o} C

Fig. 3, where it is observed that the variation of pH in terms of A can be represented by a polynomial function. Nonetheless, it is detected that for pH values below 5.1, the pH trajectories in Fig. 3 present a different behavior: at short acidification rates the decrease of pH values is faster.

According to Hofland et al. (2003), around pH values of 5.1 small particles would rapidly grow and the buffering groups of the protein and residual micellar calcium phosphate become less accessible for the added acid. This indicates that almost all caseins have precipitated, the aggregation proceeds to form bigger particles, the micellar calcium phosphate is completely depleted and the acid is being diffused in the serum (Mekmene et al., 2010). This diffusion acts similarly to a buffer which prevents the pH from getting to lower values (Hofland et al., 2003). In this context, the acid addition stage is separated into two parts: the mechanisms happening above and below pH 5.1, where pH 5.1 is the point at which the pH trajectories in Fig.3 diverge. The model for the pH values larger than 5.1 can be considered to vary according to a quadratic function in terms of A. Furthermore, temperature T is also taken into account in the sense of an Arrhenius type of equation. Regarding the part for pH below 5.1, we propose to use another quadratic function that also depends on temperature. In this case, however, we consider that the acidification time (t_A) play a role in the different mechanisms observed in Fig. 5 having an impact in the temperature and the acid addition. Hence, all the coefficients are affected by t_A. The model for pH dynamics during the acid addition stage can be written as follows:

$$\text{pH}-\text{pH}_0 = \begin{cases} (\theta_1 A^2 + \theta_2 A) e^{\left(\frac{\lambda_1}{T}\right)}, & \text{if pH} \geq 5.1 \\ \frac{(\theta_3 A^2 + \theta_4 A)}{{t_A}^{\beta_1}} e^{\left(\frac{\lambda_2}{T}\left(\frac{1}{t_A}\right)^{\beta_2}\right)}, & \text{if pH} < 5.1 \end{cases} \qquad (2)$$

where the parameters θ_{1-4} are constants expressed in pH value/min to deal with the quadratic representations of the change of pH with respect to A, whereas λ_{1-2} are constants to consider variation due to temperature (K). The parameters β_1 and β_2 are dimensionless constants allowing to adapt the model for different acidification rates. For instance, β_2 deals with the fact that at low temperatures, there is no undershoot (see Fig. 2). pH_0 is the initial pH. It is important to note that pH_0 corresponds

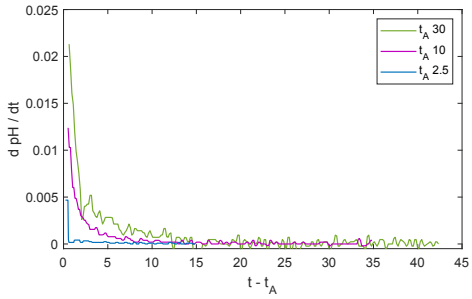

Fig. 4. pH variations after acid addition

to the third term in the quadratic polynomial function. In this case, it has been subtracted to make the regression start at the proper initial condition.

The second stage of the experiments considers a pure diffusion process involving the increase of pH to values close to the isoelectric point, where the pH values achieve equilibrium. From the experiments (Fig. 2), it is observed that the pH decreases and then stabilizes due to the action of mixing and buffering. In order to find a function that describes the changes of pH, we have plotted $\frac{d\text{pH}}{dt}$ with respect to time in Fig. 4. It can be observed that the trend follows an exponential decay that depends on t_A. Furthermore, the Arrhenius type of equation is also added to consider the variations with respect to temperature and to keep consistency with the previous stage of the model. The model for the second stage is thus expressed as:

$$\frac{d\text{pH}}{dt} = f_{diff} = \theta_5 \left(\frac{1}{t_A}\right)^{\beta_3} e^{(\theta_6\ (t-t_A))} e^{\left(\frac{\lambda_3}{T}\right)} \tag{3}$$

where θ_{5-6} are constants with dimensions pH value$/min$ and $1/min$, respectively. λ_3 is the constant to deal with temperature variations in (K). The parameter β_3 is introduced to manage the differences between acidification times.

From equations 2 and 3, it is possible to obtain the dynamics of pH by applying the chain rule of differentiation. Hence, the complete model can be expressed as:

$$\frac{d\text{pH}}{dt} = \begin{cases} \frac{\partial \text{pH}}{\partial A}\frac{\partial A}{\partial t}, & \text{if } Q > 0 \\ f_{diff}, & \text{if } Q = 0 \end{cases} \tag{4}$$

$$\frac{dA}{dt} = Q_A \tag{5}$$

where Q_A is the acid addition rate ($L_{\text{acid}}/L_{\text{milk}} - \text{min}$), whose cumulative sum is A. It is worth noting that pH_0 in the equation 2 disappears due to the chain rule derivation. It is, however, taken into account as the initial condition of ordinary differential equation 4. The dynamic model comprises two differential equations and 12 parameters to describe the change of pH varying temperatures and acidification times.

4. RESULTS

4.1 Calibration and validation of the model

The empirical model has been calibrated using the experimental data described in section 3.2. The mean values between the replicates of data in Fig. 2 have been used to build twelve data sets comprising: three temperatures ($T = 5, 20, 44^o$C) and the four acidification times ($t_A = 0, 2.5, 10, 30$ min). In order to consider $t_A = 0$, we have assumed that the acidification time was shorter than the response of the pH probe, which is lower than 9 seconds (Hofland et al., 2003). For modeling purposes, we have set $t_A = 3s$ ($t_A = 0.05$ min) when referring to $t_A = 0$ min.

Parameter identification has been performed dividing the data into acid addition stage above pH 5.1, below pH 5.1 and diffusion stage $t > t_A$. First, the parameters θ_1, θ_2 and λ_1 have been identified with only nine data sets for the values of pH ≥ 5.1. In this case, the sets for $t_A = 0$ have not been taken into account because the first two points (within a 10 seconds frame) reflect a change from the initial pH to a value already at pH 4.6 or below. A similar approach is followed for the second part, where again only nine data sets have been taken into account to estimate the parameters θ_3, θ_4 and λ_2 per t_A, considering again only the nine data sets for $t_A > 0$. Hence, three values for each parameter (θ_3, θ_4 and λ_2) have been obtained. In order to find a unique set of parameters for all T and t_A, we have proposed the correcting factors β_1 and β_2 considering the variations due to t_A. The values for β_{1-2} are first inferred from the variations of the parameters θ_3, θ_4 and γ_2. Then, a re-calibration has been made to find an optimal value for the parameters involved in $f_2(A, T, t_A)$. It is worth noting that estimating the five parameters at the same time may hamper identifiability. This was addressed by setting small bounds for the parameters β_{1-2}. Finally, the twelve data sets for $t > t_A$ has been used to identify the parameters of equation 3. Parameter identification has been performed by the pattern search method from the optimization toolbox (MATLAB 2019) in order to minimize the sum of the squared errors between the experimental data and the model outputs. The identified parameters are reported in Table 1. It is important to note that the effect of the temperature in the dynamics of pH is different after pH 5.1, which is related to the fact that at lower temperatures there is no coagulation.

The output of the model compared to the experimental data is displayed in Fig.5 for the different experimental conditions. It can be observed that the model predictions present a good fit since the pH dynamics are followed quite accurately for all the data points. The performance of the model has been evaluated by means of the Root Mean Squared Errors (RMSE). The values of the RMSE are reported for each acidification time in Table 2, where the average of the calibration errors for all data sets is about 0.05 in pH units. The standard deviations are also presented to highlight that the errors of the model can fall within a measurement error of $\pm$ 0.06 pH units.

Table 1. Parameters of the dynamic model.

		Value			Value
θ_1	[pH$/min$]	157.23	λ_1	[K]	439.31
θ_2	[pH$/min$]	-15.64	λ_2	[K]	-499.06
θ_3	[pH$/min$]	1398.2	λ_3	[K]	-3226.31
θ_4	[pH$/min$]	-291.34	β_1	[-]	0.288
θ_5	[pH$/min$]	13.77	β_2	[-]	0.15
θ_6	[$1/min$]	-0.2153	β_3	[-]	0.11

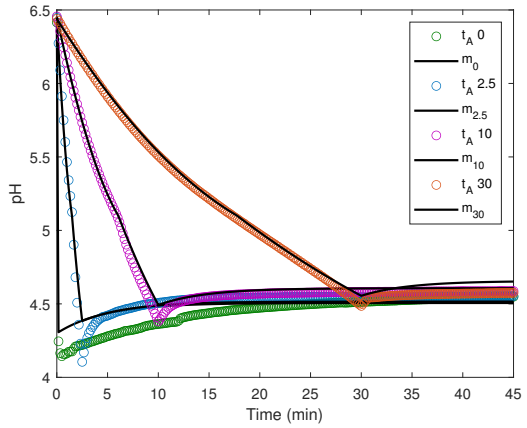

(a) 44 ^{o} C

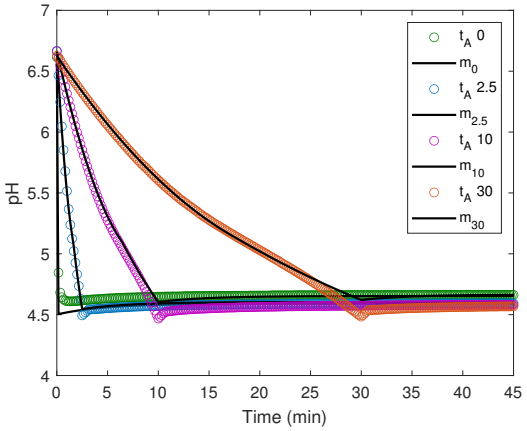

(b) 20 ^{o} C

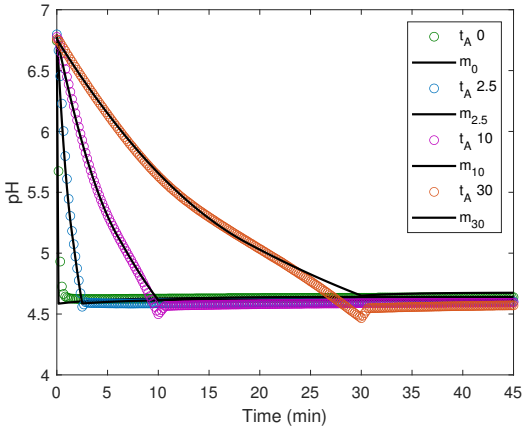

(c) 5 ^{o} C

Fig. 5. Model outputs against experimental data. Dots represent experimental data, solid lines are model outputs for the different acidification times t_A.

In order to assess the validity of the model, we have compared it against an independent data set reported in the literature (Hofland et al., 2003). This data set has been performed at similar stirring speeds, and a temperature of 40 ^{o} C. The validation results are shown in Fig.6. It is observed that the model follows the dynamic behavior of the pH. However, the model predictions fall short at

Table 2. Performance evaluation of the model with the calibration and validation data sets.

t_A (min)	RMSE Calibration	RMSE Validation	Standard Deviation
0	0.075	-	0.053
1	-	0.072	0.057
2.5	0.033	-	0.025
6	-	0.087	0.051
10	0.055	0.106	0.063
16	-	0.068	0.055
30	0.062	-	0.042

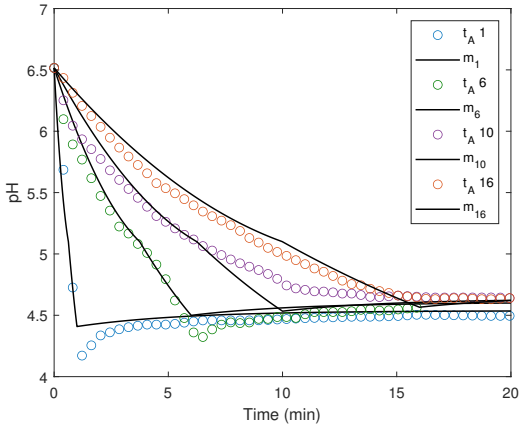

Fig. 6. Validation of the model. Data from (Hofland et al., 2003). Stirring rate 500 rpm, temperature 40^{o}C

$t_A = 10$ minutes. This can be explained by the fact that the experiments presented in section 3 were performed in flasks, whilst the ones reported in (Hofland et al., 2003) used a 1 L reactor. Hence, the stirring speed, although the same, could have different impact in a larger volume. Similarly to the experiments, the validation was assessed by the RMSE, where the values for the different data sets are low, indicating that the model is valid for the independent data set. Therefore, the model can be used to predict the dynamics of pH at different t_A and temperatures.

4.2 Advisory control of pH

The empirical model could be employed in a supervisory manner to achieve a desired pH value manipulating the acid addition rate Q_A when the temperature T and the initial pH of the milk (pH_0) are known. An optimization problem can be formulated as follows:

$$\min_{Q_A} (\text{pH} - \text{pH}_{target})^2$$

$$s.t.$$

$$Eq.(4) - (5)$$

where pH_{target} is the desired pH to be achieved after acidification. As we are interested in a set-point of pH which is attained at the end of the batch, a simple option is to define a constant Q_A and therefore, only one value for Q_A is obtained from this optimization problem.

For the sake of illustration, let us consider the case of the industrial production of casein as presented in Fig. 1 to explain the procedure of the control strategy. Industrial production is normally conducted in continuous operation

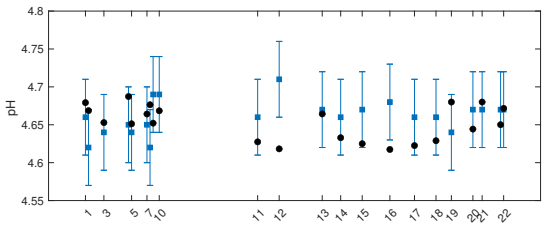

(a) Comparison of predicted pH with pH from the plant.

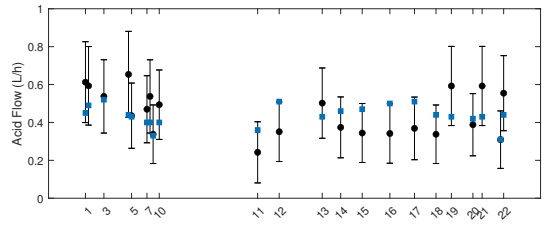

(b) Results of advisory tool against plant data.

Fig. 7. Example of Industrial application and comparison with data sampled at different days.

and thus the acid addition is fast, for which we can consider $t_A = 0$ minutes. Before using the model for industrial operation the values of the added acid per volume of milk need to be scaled to be equivalent to the lab experiments as follows:

$$A_P = \frac{Q_{A,P}}{Q_{A,Ex}} \frac{C_{A,P}}{C_{A,Ex}} \tag{6}$$

where $C_{A,P}$ and $C_{A,Ex}$, and $Q_{A,P}$ and $Q_{A,Ex}$ are to the concentrations of the acid and the acid addition rates in the plant P and the experiments Ex, respectively. The term A_P holds for the cumulative added acid per volume of milk in the plant. Once the acid addition has been scaled up, the model must be verified against plant values to assess its performance. If deviations are observed, a re-calibration of parameters must be performed to cope with the different conditions between the experiments for which the model has been designed and the actual plant.

Considering that the model has been well adapted to the plant, the optimization problem is solved to obtain the acid addition rate Q_A at every time that the values of T and pH_0 are changed. An example of the validation of the model with plant data is displayed in Fig. 7(a), where it is observed that the model is able to predict the pH within the measurement error of ± 0.05 in 90% of 22 samples. The results of the optimization (Q_A) to attain a $pH_{target} = 4.65$ is displayed in Fig. 7(b), where the values of acid flow are normalized to 1. In this case, the optimization was implemented for a given set of pH of milk pH_0, flow of milk Q_M, temperature T and pH_{target}. Since the pH measurements have an error of $\pm$ 0.05, 500 Monte Carlo simulations were carried out to consider a normal distribution with mean pH_0 and standard deviation of $\pm$ 0.05. The predictions of the suggested acid flow by the optimization are in line with the ones that the operators use to control the pH.

5. CONCLUSIONS

This work has presented a model to describe the dynamics of pH during acidification of milk for the precipitation of acid casein. The model has been found accurate to predict the pH at different acidification times and temperatures. Furthermore, we have proposed a case study where the model could be employed using an optimization routine to provide an indication, in a supervisory manner, about the acid flow required to keep the pH at a desired value. This case is only illustrative, but it intends to highlight a potential application of the model. Further extensions of the model can be envisaged, such as the prediction of the dynamics of calcium and phosphates in the whey, and the adaptation for the acidification of other dairy products (*i.e.* yogurt).

ACKNOWLEDGEMENTS

This work is part of the INSPEC project (Integrating Sensor Based Process Monitoring and Advanced Process Control) managed by the Institute for Sustainable Process Technology (ISPT) and co-funded by TKI-E & I with the supplementary grant 'TKI- Toeslag' for Topconsortia for Knowledge and Innovation (TKI's) of the Ministry of Economic Affairs and Climate Policy.

REFERENCES

Bringe, N.A. and Kinsella, J.E. (1990). Acidic coagulation of casein micelles: Mechanisms inferred from spectrophotometric studies. *Journal of Dairy Research*, 57(3), 365–375. doi: 10.1017/S0022029900027023.

De Kruif, C.G. (1997). Skim milk acidification. *Journal of Colloid and Interface Science*, 185(1), 19–25. doi:10.1006/jcis.1996.4548.

Fox, N.I. (2011). A tall tower study of Missouri winds. *Renewable Energy*, 36(1), 330–337. doi:10.1016/j.renene.2010.06.047.

Hofland, G.W., Berkhoff, M.R., Witkamp, G.J., and Van der Wielen, L.A. (2003). Dynamics of isoelectric precipitation of casein using sulfuric acid. *AIChE Journal*, 49(8), 2211–2223. doi: 10.1002/aic.690490828.

Holt, C. (2004). An equilibrium thermodynamic model of the sequestration of calcium phosphate by casein micelles and its application to the calculation of the partition of salts in milk. *European Biophysics Journal*, 33(5), 421–434. doi:10.1007/s00249-003-0377-9.

Holt, C., Dalgleish, D.G., and Jenness, R. (1981). Calculation of the ion equilibria in milk diffusate and comparison with experiment. *Analytical Biochemistry*, 113(1), 154–163. doi:10.1016/0003-2697(81)90059-2.

Jablonka, M.S., Munro, P.A., and Crabbe, P.G. (1986). Effect of precipitation temperature and pH on the mechanica strength of batch precipitated acid casein curd. *Journal of Dairy Research*, 53, 69–73.

Lucey, J.A. (2017). Formation, Structural Properties, and Rheology of Acid-Coagulated Milk Gels. In *Cheese: Chemistry, Physics and Microbiology: Fourth Edition*, volume 1, 179–197. Elsevier Inc. doi:10.1016/B978-0-12-417012-4.00007-7.

Mekmene, O., Le Graët, Y., and Gaucheron, F. (2009). A model for predicting salt equilibria in milk and mineral-enriched milks. *Food Chemistry*, 116(1), 233–239. doi:10.1016/j.foodchem.2009.02.039.

Mekmene, O., Le Graët, Y., and Gaucheron, F. (2010). Theoretical model for calculating ionic equilibria in milk as a function of pH: Comparison to experiment. *Journal of Agricultural and Food Chemistry*, 58(7), 4440–4447. doi:10.1021/jf903628r.

Mudgil, D. and Barak, S. (2019). Dairy-based functional beverages. In *Milk-Based Beverages: Volume 9: The Science of Beverages*, 67–93. Elsevier. doi:10.1016/B978-0-12-815504-2.00003-7.

Sarode, A.R., Sawale, P.D., Khedkar, C.D., Kalyankar, S.D., and Pawshe, R.D. (2015). Casein and Caseinate: Methods of Manufacture. *Encyclopedia of Food and Health*, 676–682. doi: 10.1016/B978-0-12-384947-2.00122-7.

TetraPack (2015). Casein. In *Dairy Processing Handbook*, Chapter 20. TetraPack. doi:https://www.tetrapak.com/about/tetra-pak-dairy-processing-handbook.